

PNAS



1

2 **Supporting Information for**

3 **Self-propulsion via slipping: frictional swimming in multi-legged locomotors**

4 **Baxi Chong, Juntao He, Shengkai Li, Eva Erickson, Kelimar Diaz, Tianyu Wang, Daniel Soto, Daniel I Goldman**

5 **Daniel I Goldman**

6 **E-mail: daniel.goldman@physics.gatech.edu**

7 **This PDF file includes:**

- 8 Figs. S1 to S4
- 9 Legend for Movie S1
- 10 SI References

11 **Other supporting materials for this manuscript include the following:**

- 12 Movie S1

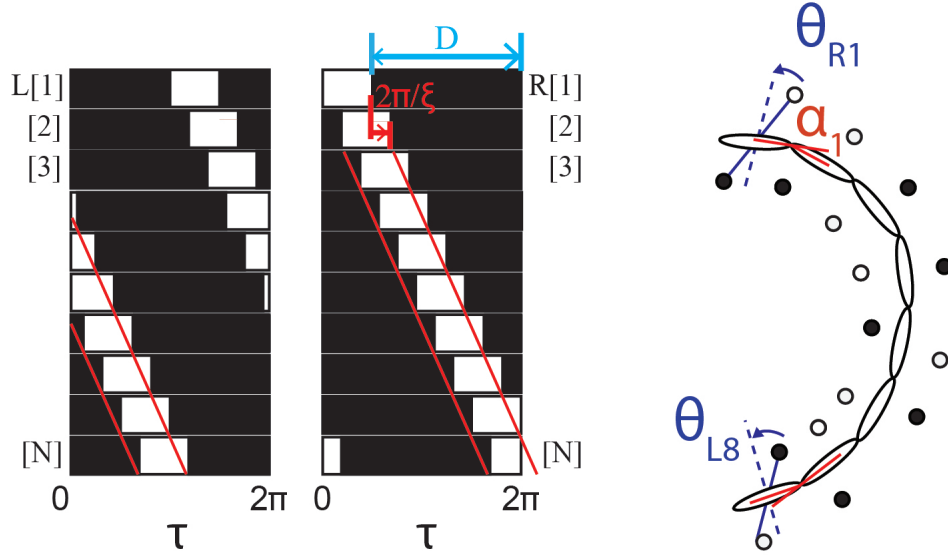


Fig. S1. Gait prescription The joint angles and contact states definition. In the contact sequence diagrams, filled blocks represent stance phase, and open blocks represent swing phase. The blue arrow represents the duty factor D . The red arrow represents the phase lag between consecutive modules. τ denote gait phase.

1. Supplementary movie caption

Movie S1. 0:04-0:25, friction coefficient independency. 0:26-0:36, temporal frequency independency. 0:37-0:51, effective viscous drag. 0:52-1:55, performance space. 1:56-2:09, obstacles-rich environments. 2:10-2:18, biological centipedes.

2. Text

Gait prescription of multi-legged robots. We use a binary variable c to represent the contact state of a leg, where $c = 1$ represents the stance phase and $c = 0$ represents the swing phase. Following (1), the contact pattern of symmetric quadrupedal gaits can be written as

$$\begin{aligned}
 c_l(\tau_c, 1) &= \begin{cases} 1, & \text{if } \text{mod}(\tau_c, 2\pi) < 2\pi D \\ 0, & \text{otherwise} \end{cases} \\
 c_l(\tau_c, i) &= c_l(\tau_c - 2\pi \frac{\xi}{n}(i-1), 1) \\
 c_r(\tau_c, i) &= c_l(\tau_c + \pi, i), \tag{1}
 \end{aligned}$$

where ξ denotes the number of spatial waves on legs, D the duty factor, $c_l(\tau_c, i)$ (and $c_r(\tau_c, i)$) denotes the contact state of i -th leg on the left (and the right) at gait phase τ_c , $i \in \{1, \dots, n\}$ for $2n$ -legged systems.

Legs generate self-propulsion by protracting during the stance phase to make contact with the environment, and retracting during the swing phase to break contact. That is, the leg moves from the anterior to the posterior end during the stance phase and moves from the posterior to anterior end during the swing phase. With this in mind, we use a piece-wise sinusoidal function to prescribe the anterior/posterior excursion angles (θ) for a given contact phase (τ_c) defined earlier,

$$\begin{aligned}
 \theta_l(\tau_c, 1) &= \begin{cases} \Theta_{leg} \cos(\frac{\tau_c}{2D}), & \text{if } \text{mod}(\tau_c, 2\pi) < 2\pi D \\ -\Theta_{leg} \cos(\frac{\tau_c - 2\pi D}{2(1-D)}), & \text{otherwise,} \end{cases} \\
 \theta_l(\tau_c, i) &= \theta_l(\tau_c - 2\pi \frac{\xi}{n}(i-1), 1) \\
 \theta_r(\tau_c, i) &= \theta_l(\tau_c + \pi, i) \tag{2}
 \end{aligned}$$

where Θ_{leg} is the shoulder angle amplitude, $\theta_l(\tau_c, i)$ and $\theta_r(\tau_c, i)$ denote the leg shoulder angle of i -th left and right leg at contact phase τ_c , respectively. Note that the shoulder angle is maximum ($\theta = A_\theta$) at the transition from swing to stance phase, and is minimum ($\theta = -A_\theta$) at the transition from stance to swing phase.

We then introduced the lateral body undulation by propagating a wave along the backbone from head to tail, The body undulation wave is

$$\alpha(\tau_b, i) = \Theta_{body} \cos(\tau_b - 2\pi \frac{\xi^b}{n}(i-1)), \tag{3}$$

26 where $\alpha(\tau_b, i)$ is the angle of i -th body joint at phase τ_b , ξ^b denotes the number of spatial waves on body. For simplicity, we
 27 assume that the spatial frequency of the body undulation wave and the contact pattern wave are the same, i.e. $\xi^b = \xi$. In this
 28 way, gaits of multi-legged locomotors by superposition of a body wave and a leg wave can be described as the phase of contact,
 29 ϕ_c , and the phase of lateral body undulation τ_b .

30 We quantified the body-leg coordination by its phase lag: $\phi_{bc} : \phi_c - \tau_b$. As discussed in (1), the optimal body-leg coordination
 31 (optimal phasing of body undulation to assist leg retraction) is $\phi_{bc} \sim -(\xi/N + 1/2)\pi$.

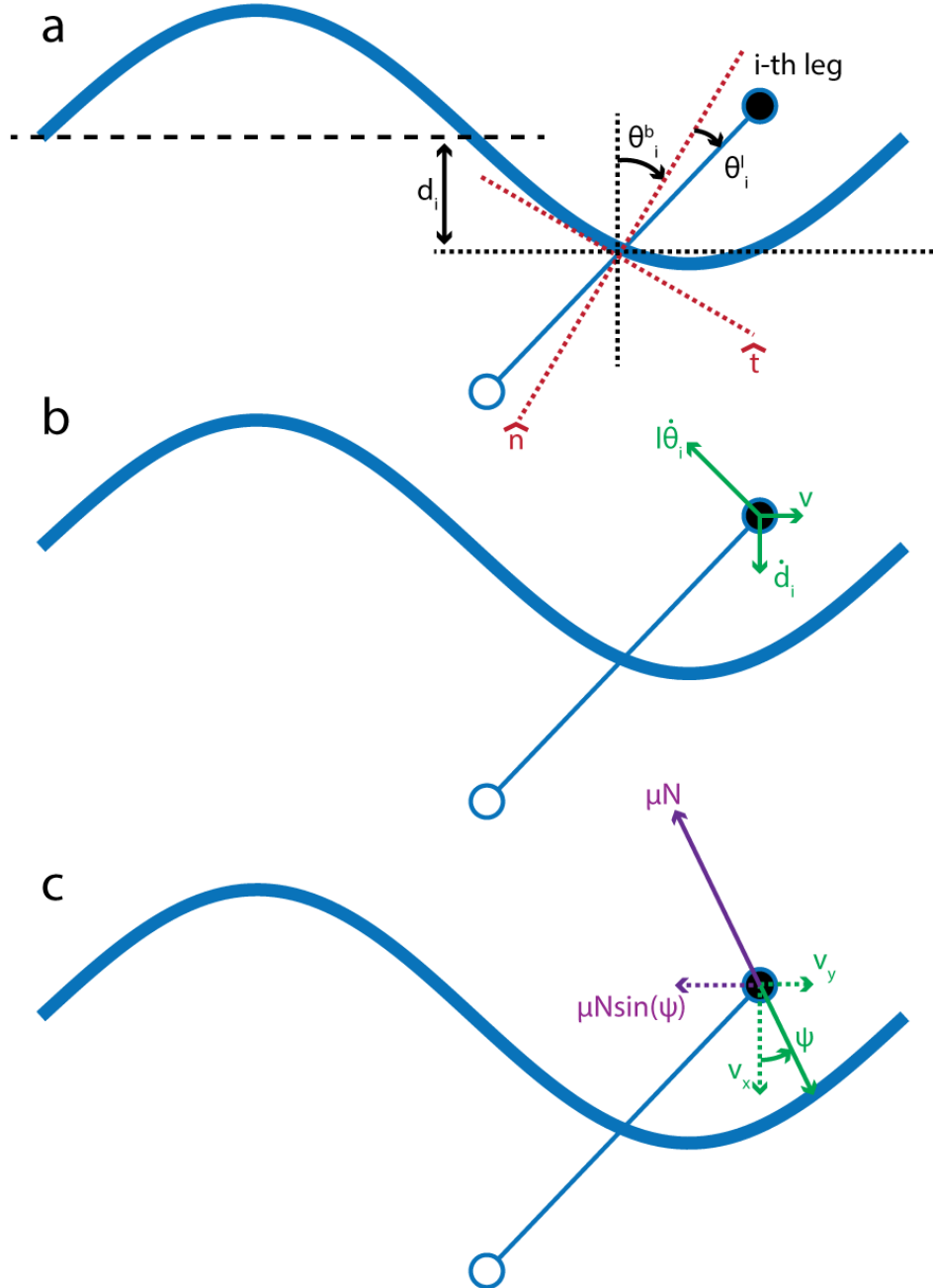


Fig. S2. (a) The orientational and lateral oscillation. (b) Components of velocity on a leg (c) Reaction force on a leg

32 **Kinematic model.** As reported in prior work, the undulatory body will experience orientational and lateral oscillation:

$$d = d_m \sin \tau$$

$$\theta^b = \theta_m^b \cos \tau$$

33 The leg protraction and retraction will contribute to increase the orientational oscillation:

$$\theta = \theta^b + \theta_m^l \cos(\tau).$$

34 The derivative of orientational and lateral oscillation can cause slipping of the leg. There are three components of leg
 35 slipping velocity: the one from CoG (center of geometry) translation (v), the one from lateral oscillation (d), the one from
 36 angular velocity ($l\dot{\theta}$). From geometry, we can have Eq. 2 in the main text (shown below).

$$\begin{aligned} v_x(\tau) &= \dot{d}(\tau) + l\dot{\theta}(\tau) \sin(\theta(\tau)) \\ v_y(\tau, v) &= v + l\dot{\theta}(\tau) \cos(\theta(\tau)) \end{aligned}$$

37 In Coulomb friction model, the magnitude of friction should be independent of the magnitude of slipping. Instead, it should
 38 only depend on the direction of slipping, Ψ . We can calculate Ψ by:

$$\psi(\tau) = \tan^{-1}\left(\frac{v_y(\tau, v)}{v_x(\tau)}\right)$$

39 The projection of the friction into y -axis is given by:

$$f_y(\tau, v) = -\mu N \sin(\psi(\tau))$$

40 **Dynamic model.** As discussed in Eq. 2, the ground reaction force acting on i -th module (a pair of legs and a body connection
 41 unit) is given by:

$$f_y^i(\tau, v) = -\mu N \sin\left(\tan^{-1}\left(\frac{v_y(\tau, v)}{v_x(\tau)}\right)\right) \quad [4]$$

42 Thus, the total force acting on the n -link robot is:

$$f_y^{all}(\tau, v) = -\mu N \sum_{i=0}^{n-1} \sin\left(\tan^{-1}\left(\frac{v_y(\tau + 2\pi\frac{\xi}{n}i, v)}{v_x(\tau + 2\pi\frac{\xi}{n}i)}\right)\right) \quad [5]$$

43 Now we replace τ as $2\pi ft$ (t is time), N as mg/n (m is the mass of the robot), f_y^{all} as $-m\dot{v}$, we have:

$$\dot{v}(t, v) = \frac{\mu g}{n} \sum_{i=0}^{n-1} \sin\left(\tan^{-1}\left(\frac{v_y(2\pi ft + 2\pi\frac{\xi}{n}i, v)}{v_x(2\pi ft + 2\pi\frac{\xi}{n}i)}\right)\right), \quad [6]$$

44 which we can solve numerically to get the dynamic simulation.

45 **Lego field built up.** We built up an obstacle rich environment using Lego blocks. First, we divided an 150cm \times 90cm area of a
 46 wooden sheet into 1.5cm \times 1.5cm squares (100 blocks along the length, 60 blocks along the width). The distribution of those
 47 Lego bricks* were generated by MATLAB *rand()* function. Specifically, we used *rand()* to create a 100 \times 60 matrix with
 48 uniformly distributed random variable. We marked the row and column information for the entries with highest 120 values.
 49 We placed the Lego bricks to the designated position. Finally, we hot glued Lego bricks on planned positions. The final layout
 50 of the Lego field is shown in Figure.S3.

*Included in LEGO Classic Large Creative Brick Box: <https://www.lego.com/en-us/product/lego-large-creative-brick-box-10698>



Fig. S3. Lego field: 120 Lego bricks(1.5cm × 1.5cm × 1cm) were randomly placed in an 150cm × 90cm area. Their distribution was generated by uniformly distribution.

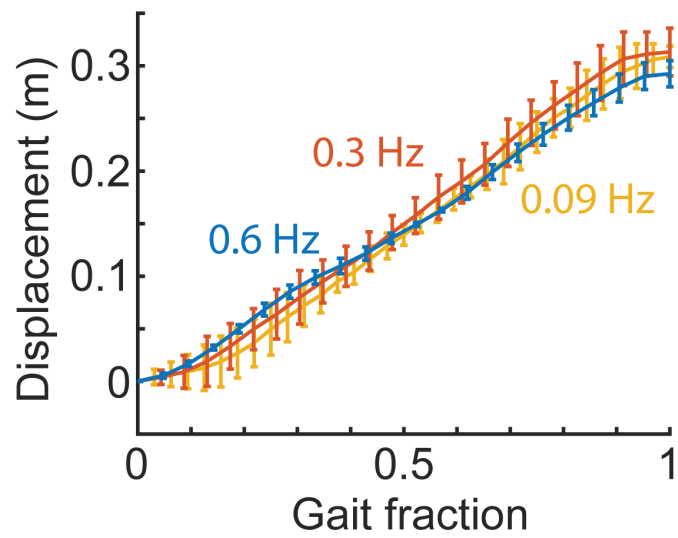


Fig. S4. Temporal frequency Independence Robot ($n = 6$) implementing the same gait ($\Theta_{body} = \pi/3, \Theta_{leg} = 0$) under different temporal frequencies. The development of CoG displacement as a function of gait fraction under different temporal frequencies.

51 **References**

- 52 1. B Chong, et al., A general locomotion control framework for multi-legged locomotors. *Bioinspiration & Biomimetics* **17**,
53 046015 (2022).